

From pseudo-direct hexagonal germanium to direct silicon-germanium alloys

Pedro Borlido, Jens Renè Suckert, Jürgen Furthmüller, Friedhelm Bechstedt, Silvana Botti, Claudia Rödl

Institut für Festkörpertheorie und -optik, Friedrich-Schiller-Universität Jena, Max-Wien-Platz 1, 07743 Jena, Germany and European Theoretical Spectroscopy Facility

Abstract

We present *ab initio* calculations of the electronic and optical properties of hexagonal $\text{Si}_x\text{Ge}_{1-x}$ alloys in the lonsdaleite structure. Lattice constants and electronic band structures in excellent agreement with experiment are obtained using density-functional theory. Hexagonal Si has an indirect band gap, while hexagonal Ge has a pseudo-direct gap, i.e. the optical transitions at the minimum direct band gap are very weak. The pseudo-direct character of pure hexagonal Ge is efficiently lifted by alloying. Already for a small admixture of Si, symmetry reduction enhances the oscillator strength of the lowest direct optical transitions. The band gap is direct for a Si content below 45%. We validate lonsdaleite group-IV alloys to be efficient optical emitters, suitable for integrated optoelectronic applications.

Keywords: semiconductors, optical materials, electronic band structure, optical properties, computer simulations

1. Introduction

Alloys of silicon (Si) and germanium (Ge) in the diamond crystal structure with a molar fraction x of Si and $(1-x)$ of Ge, i.e., $\text{Si}_x\text{Ge}_{1-x}$, are commonly used as semiconductor materials in integrated circuits, as heterojunction bipolar transistors, or as strained layers in CMOS transistors [1]. These $\text{Si}_x\text{Ge}_{1-x}$ alloys are indirect semiconductors and, hence, not optimal for use in active optoelectronic devices, such as photonic integrated chips [2]. Therefore, over the past years, a lot of effort has been devoted to engineer group-IV materials (and their alloys) with direct gaps and strong dipole-active optical transitions at the minimum band gap by straining, nanostructuring or amorphization [3, 4, 5, 6, 7, 8].

At present, the hexagonal (hex) lonsdaleite phase $P6_3/mmc (D_{6h}^4)$ of group-IV semiconductors is attracting growing attention. The backfolding of the conduction-band minima of the cubic phase from the L points onto the Γ point of the hexagonal Brillouin zone renders hex-Ge a direct semiconductor [9]. However, this direct band gap has a pseudo-direct character, as optical transitions at the lowest gap are very weak. Hex-Si, instead, re-

mains an indirect semiconductor [10, 9], since another band minimum at the M point is situated at lower energy than the backfolded minimum at Γ . Lonsdaleite group-IV materials have been fabricated using ultraviolet laser ablation [11, 12] or the crystal-phase transfer method [13, 14]. Recently, hex-Si and hex-Ge have been realized growing on templates of wurtzite GaP nanowires in form of core-shell nanowires [15, 8] with high crystal quality [16].

The first theoretical study of hex- $\text{Si}_x\text{Ge}_{1-x}$, using a virtual-crystal approximation, suggested a direct-indirect gap crossover for intermediate compositions [17] and negative direct gaps for Ge-rich alloys. The precise composition x of this crossover and the strength of the lowest-energy optical transitions over the whole composition range remain important open questions which will be addressed in the present work.

2. Methods

We have performed density-functional theory (DFT) calculations using the VASP package [18] with the projector-augmented wave method [19] and a plane-wave cutoff of 500 eV, treating the shallow Ge $3d$ electrons

as valence electrons. For geometry optimization, we have employed the PBEsol [20] exchange-correlation functional, which gives accurate results for lattice parameters of solids [21, 22]. The Brillouin zone integration was performed using Γ -centered \mathbf{k} -point grids with a density equivalent to a $12 \times 12 \times 6$ mesh for the primitive lonsdaleite unit cell (approximately 5000 points per reciprocal atom [23]). Atomic geometries were relaxed until the forces on the atoms were smaller than 1 meV/Å.

Accurate band structures were computed using the modified Becke-Johnson exchange-correlation potential [24], including spin-orbit coupling. Previous work has proven excellent agreement with experiment for the band gaps of semiconductors [25] and, in particular, cubic as well as hexagonal Si and Ge [26, 10, 9].

In addition to the band gaps, we also study the radiative lifetime τ as a global measure of the light-emission properties. To this end, we compute the radiative recombination rate $A_{c\mathbf{v}\mathbf{k}}$ for vertical optical transitions between a conduction state $|c\mathbf{k}\rangle$ and a valence state $|v\mathbf{k}\rangle$ with the one-particle energies $\varepsilon_{c\mathbf{k}}$ and $\varepsilon_{v\mathbf{k}}$ as [27, 28]

$$A_{c\mathbf{v}\mathbf{k}} = n_{\text{eff}} \frac{e^2(\varepsilon_{c\mathbf{k}} - \varepsilon_{v\mathbf{k}})}{\pi \epsilon_0 \hbar^2 m^2 c^3} \frac{1}{3} \sum_{j=1}^3 | \langle c\mathbf{k} | p_j | v\mathbf{k} \rangle |^2, \quad (1)$$

with n_{eff} the effective refractive index of the medium. The squares of the momentum matrix elements $\langle c\mathbf{k} | p_j | v\mathbf{k} \rangle$ are averaged over the Cartesian directions, corresponding to the emission of unpolarized light. The decay rate $1/\tau$ can then be approximated as the thermal average of the recombination rates at temperature T ,

$$\frac{1}{\tau} = \sum_{c\mathbf{v}\mathbf{k}} A_{c\mathbf{v}\mathbf{k}} \frac{w_{\mathbf{k}} e^{-(\varepsilon_{c\mathbf{k}} - \varepsilon_{v\mathbf{k}})/(k_B T)}}{\sum_{c'\mathbf{v}'\mathbf{k}'} w_{\mathbf{k}'} e^{-(\varepsilon_{c'\mathbf{k}'} - \varepsilon_{v'\mathbf{k}'})/(k_B T)}} \quad (2)$$

with the \mathbf{k} -point weights $w_{\mathbf{k}}$. The direction-averaged refractive indices of hex-Si and hex-Ge are 3.2 and 3.7. As in cubic $\text{Si}_x\text{Ge}_{1-x}$ alloys [29], a smooth, but not linear variation can be expected for intermediate compositions. For not introducing a bias in absence of data for the intermediate compositions, we plot $1/(\tau n_{\text{eff}})$.

We describe $\text{Si}_x\text{Ge}_{1-x}$ alloys by a cluster expansion within the strict-regular-solution (SRS) model [30, 31]. Using the GENSTR tool of the ATAT package [32], we constructed all ordered $\text{Si}_x\text{Ge}_{1-x}$ structures representable by

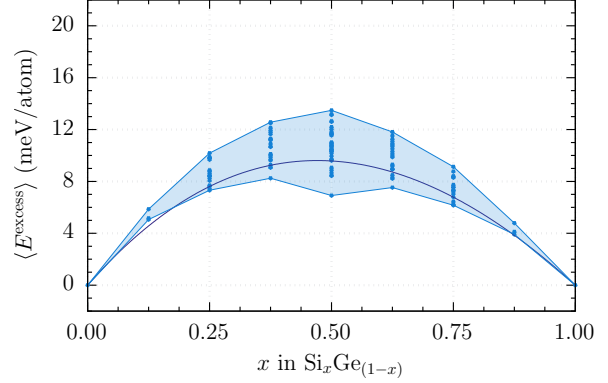


Figure 1: Alloy-averaged excess energy $\langle E^{\text{excess}} \rangle(x)$ of hex- $\text{Si}_x\text{Ge}_{1-x}$ as a function of composition (solid line). Dots indicate the excess energies E_j^{excess} of the individual clusters, with the spread of values at each composition highlighted by the shaded region.

8-atom supercells (clusters) resulting in 118 symmetry-inequivalent clusters of 3 different cell shapes. Any thermodynamic property $\langle D \rangle(x)$ of the alloy can then be written as a weighted average over the cluster properties D_j . Within the SRS model, the alloy average translates into $\langle D \rangle(x) = \sum_j x_j^0 D_j$, with the weights $x_j^0 = g_j(1-x)^{n-n_j}x^{n_j}$ of an ideal random alloy. Here, n is the total number of atoms and n_j the number of Si atoms in the cluster cell j . The number of symmetry-equivalent atomic configurations represented by each cluster is given by the degeneracy g_j . We found cluster sizes of $n = 8$ atoms sufficient for converged alloy properties.

3. Results and Discussion

3.1. Atomic structure

In Fig. 1, we show the calculated cluster excess energies

$$E_j^{\text{excess}} = E_j - \frac{n_j}{n} E_{\text{Si}} - \left(1 - \frac{n_j}{n}\right) E_{\text{Ge}}, \quad (3)$$

where E_j is the total energy of cluster j and E_{Si} and E_{Ge} are the total energies of the end components, for the 8-atom cluster cells. What is more, also the alloy-averaged excess energy $\langle E^{\text{excess}} \rangle(x)$ is plotted. All cluster excess energies are positive, as the creation of the Si-Ge bond requires energy. The largest spread of values

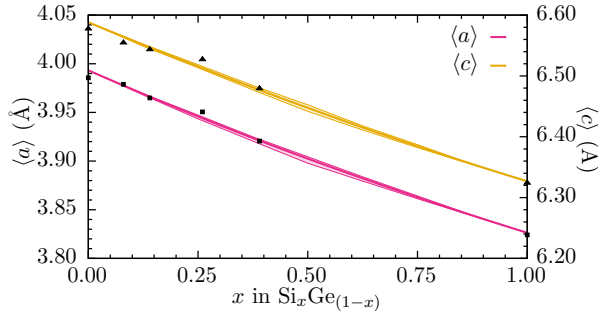


Figure 2: Lattice parameters $\langle a \rangle(x)$ and $\langle c \rangle(x)$ of hex- $\text{Si}_x\text{Ge}_{1-x}$ alloys. The very narrow shaded regions indicate the range of lattice constants obtained for the individual clusters at a given composition. Solid squares and triangles represent experimental values [13, 8] for a and c , respectively. Experimental error bars are smaller than the used symbols.

occurs for clusters with stoichiometry $n_j/n = 0.5$, ranging from 7 meV/atom to 14 meV/atom. The distribution of the excess energies is slightly asymmetric, increasing faster in the Ge-rich region, and it reaches a maximum of 9.6 meV/atom at $x = 0.47$, which is well below the thermal energy at room temperature. This implies that hex- $\text{Si}_x\text{Ge}_{1-x}$ can be treated as ideal random alloy at room temperature, and the SRS model is a justified approximation under these conditions. At lower temperatures, when thermal energies become comparable to the excess energies, more sophisticated alloy statistics, such as the generalized quasichemical approximation [30, 31], are necessary.

The lattice constants a and c of hex- $\text{Si}_x\text{Ge}_{1-x}$ are shown in Fig. 2. They vary almost linearly between $a = 3.993 \text{ \AA}$ ($c = 6.588 \text{ \AA}$) for pure Ge and $a = 3.826 \text{ \AA}$ ($c = 6.327 \text{ \AA}$) for pure Si, which is in agreement with Vegard’s law [33]. The alloy-averaged lattice parameters ($D = a, c$) can be fitted to parabolas

$$\langle D \rangle(x) = xD_{\text{Si}} + (1-x)D_{\text{Ge}} - x(1-x)b_D, \quad (4)$$

with small bowing parameters $b_a = 0.029 \text{ \AA}$ and $b_c = 0.040 \text{ \AA}$. The computed values are in excellent agreement with experimental data from x-ray diffraction [8, 34].

3.2. Electronic Structure

For optoelectronic applications, the light-emission properties of the hex- $\text{Si}_x\text{Ge}_{1-x}$ are of utmost importance.

As excited electrons will accumulate in the lowest-energy valleys of the alloy, the clusters with the smallest gap at a given composition are particularly relevant in this context. In Fig. 3, the unfolded band structures of the lowest-gap clusters with stoichiometries $n_j/n = 0.25$ and $n_j/n = 0.5$ are shown along with the band structures of hex-Si and hex-Ge. The 8-atom cluster cells were unfolded onto the lonsdaleite Brillouin zone using FOLD2BLOCH [35]. The intensity of the blue tone is proportional to the Bloch spectral weight of each state [35, 36]. It is clearly visible that the fundamental gap is direct for the lowest-gap clusters with $n_j/n = 0.25$. The lowest-gap cluster with $n_j/n = 0.5$ has an indirect gap. The overall dispersion of the bands remains largely unaffected by stoichiometry and individual bands can still be identified, despite the disorder effects due to alloying. The valence-band maximum is located at the Γ point for all clusters. The conduction-band minimum at Γ , on the other hand, is very sensitive to the composition of the alloy and shifts over a comparably wide range of values, opening the way to tune the band gap of hex- $\text{Si}_x\text{Ge}_{1-x}$ via composition engineering.

In Fig. 4(a), we trace the evolution of the alloy-averaged conduction-band minima at the most relevant high-symmetry points Γ , M , L and U (which is close to $2/3$ of the \overline{ML} line [37, 9]) from hex-Ge (Γ - Γ gap of 0.3 eV) to hex-Si (Γ - Γ gap of 1.6 eV, Γ - M gap of 1.1 eV). The alloy-averaged gap increases with increasing x and is direct for the Ge-rich compositions with $x < 0.45$. For larger x , an indirect Γ - U or Γ - M fundamental gap appears, depending on the composition. At the direct-to-indirect transition, the gap is about 0.85 eV. If, in view of discussing emission properties, we consider the lowest-gap clusters at a given composition instead of the alloy average, the direct-to-indirect transition already takes place at $x \approx 0.375$, at a gap energy of about 0.63 eV.

3.3. Radiative Lifetimes

To provide a global measure for the light-emission efficiency of hex- $\text{Si}_x\text{Ge}_{1-x}$ alloys, we calculate the alloy average $\langle 1/\tau \rangle^{-1}(x)$ of the radiative lifetime from Eq. (2) at $T = 300 \text{ K}$ (see Fig. 4(b)). Hex-Ge is a pseudo-direct semiconductor, as optical transitions between the top valence and the lowest conduction band are very weak [38, 9, 39], resulting in long radiative lifetimes (about 10^{-4} s at 300 K). However, transitions involving the second conduction band at about 0.6 eV from the top

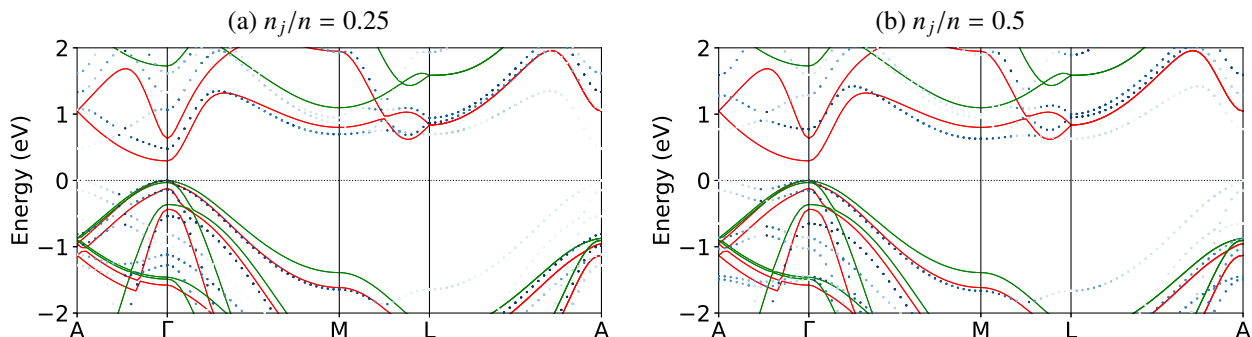


Figure 3: Band structures of hex- $\text{Si}_x\text{Ge}_{1-x}$ clusters with $n_j/n = 0.25$ and $n_j/n = 0.5$. We plot the unfolded band structure of the 8-atom cluster cell with the lowest gap (blue dots) for each composition, as well as the band structures of hex-Si (green) and hex-Ge (red) as a guide to the eye.

valence have much higher oscillator strengths, comparable to direct III-V semiconductors such as GaAs [8]. It has been predicted that moderate tensile uniaxial strain inverts the conduction-band ordering and reduces the radiative lifetime of hex-Ge by more than 3 orders of magnitude [38].

In hex- $\text{Si}_x\text{Ge}_{1-x}$ alloys, disorder reduces the crystal symmetry such that high light-emission efficiency is possible even without straining the material, since the lowest Γ - Γ transition becomes strongly dipole active for some clusters within the alloy. As is evident from Fig. 4(b), this results in an alloy-averaged radiative lifetime that is, throughout the entire range of compositions, 3 orders of magnitude lower than the lifetimes of the end components. As Eq. (1) takes only vertical transitions into account, the direct-to-indirect gap transition is not apparent in the lifetimes. However, combining the information on the direct-to-indirect gap transition from Fig. 4(a) with the strongly increased optical matrix element for vertical transitions (i.e. the by orders of magnitude reduced radiative lifetime) from Fig. 4(b), we can conclude that hex- $\text{Si}_x\text{Ge}_{1-x}$ alloys in the composition range $0 < x < 0.4$ are efficient light emitters suitable for optoelectronic applications with tunable band gaps in the spectral range of optical telecommunication.

4. Summary and Conclusions

In summary, we performed a comprehensive *ab initio* study of the electronic and optical properties of hex- $\text{Si}_x\text{Ge}_{1-x}$ alloys in view of their light-emission capabili-

ties. We verified that hex- $\text{Si}_x\text{Ge}_{1-x}$ can be described as ideal random alloy at room temperature and that the lattice parameters closely obey Vegard's law. We have shown that Ge-rich hex- $\text{Si}_x\text{Ge}_{1-x}$ alloys can be efficient optical emitters, in contrast to pure hex-Si or hex-Ge. Alloying breaks the crystal symmetry and transforms the pseudo-direct gap of hex-Ge into a strongly dipole active direct gap for the Ge-rich compositions. Overall, the electronic properties of hexagonal group-IV alloys make them very promising for active optoelectronic applications, and will surely keep attracting a fair amount of research in the near future.

Declaration of Competing Interest

The authors declare that they have no known competing financial interests or personal relationships that could have appeared to influence the work reported in this paper.

Acknowledgements

We acknowledge support from the EU through the H2020-FETOpen project SiLAS (grant agreement No. 735008). C.R. acknowledges support from the Marie Skłodowska-Curie Actions (grant agreement No. 751823). Computing time was granted by the Leibniz Centre on SuperMUC (No. pr62ja).

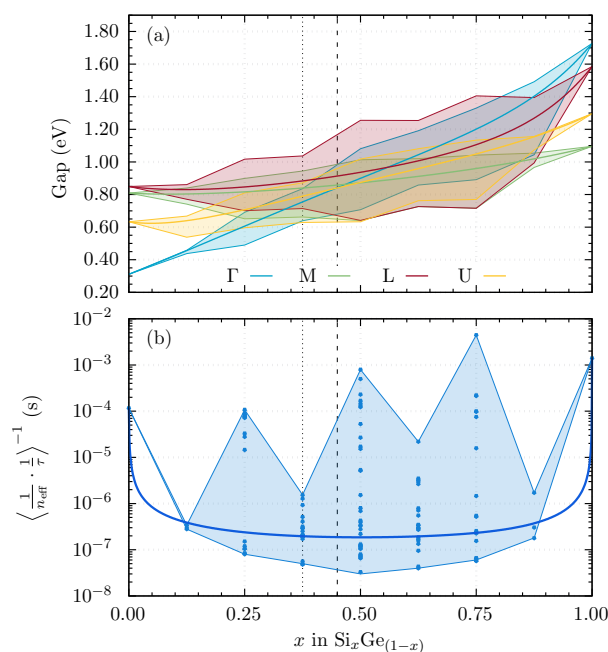


Figure 4: (a) Alloy-averaged band gaps as a function of composition. Shaded regions show the range of gap values obtained for the individual clusters at a given composition. Vertical dashed (dotted) lines indicate the direct-to-indirect gap transition for the random alloy (the lowest-gap clusters). (b) Radiative lifetime as a function of composition (solid line). Dots indicate the results for the individual clusters, with the range at each composition highlighted by the shaded region.

References

- [1] J. D. Cressler, G. Niu, Silicon-Germanium Heterojunction Bipolar Transistors, Artech House, Boston, MA, 2003.
- [2] A. H. Atabaki, S. Moazeni, F. Pavanello, H. Gevorgyan, J. Notaros, L. Alloatti, M. T. Wade, C. Sun, S. A. Kruger, H. Meng, K. Al Qubaisi, I. Wang, B. Zhang, A. Khilo, C. V. Baiocco, M. A. Popović, V. M. Stojanović, R. J. Ram, Integrating photonics with silicon nanoelectronics for the next generation of systems on a chip, *Nature* 556 (7701) (2018) 349–354. doi:10.1038/s41586-018-0028-z.
- [3] P. Ball, Let there be light, *Nature* 409 (6823) (2001) 974–976. doi:10.1038/35059301.
- [4] L. Vincent, G. Patriarche, G. Hallais, C. Renard, C. Gardès, D. Troadec, D. Bouchier, Novel heterostructured ge nanowires based on polytype transformation, *Nano Lett.* 14 (8) (2014) 4828–4836. doi:10.1021/nl502049a. URL <https://doi.org/10.1021/nl502049a>
- [5] H. I. T. Hauge, M. A. Verheijen, S. Conesa-Boj, T. Etzelstorfer, M. Watzinger, D. Kriegner, I. Zardo, C. Fasolato, F. Capitani, P. Postorino, S. Kölling, A. Li, S. Assali, J. Stangl, E. P. A. M. Bakkers, Hexagonal silicon realized, *Nano Lett.* 15 (9) (2015) 5855. doi:10.1021/acs.nanolett.5b01939. URL <https://doi.org/10.1021/acs.nanolett.5b01939>
- [6] S. Assali, M. Albani, R. Bergamaschini, M. A. Verheijen, A. Li, S. Kölling, L. Gagliano, E. P. Bakkers, L. Miglio, Strain engineering in ge/gesn core/shell nanowires, *Appl. Phys. Lett.* 115 (11) (2019) 113102. doi:10.1063/1.5111872.
- [7] H. I. T. Hauge, S. Conesa-Boj, M. A. Verheijen, S. Koelling, E. P. A. M. Bakkers, Single-crystalline hexagonal silicon-germanium, *Nano Lett.* 17 (1) (2017) 85–90. doi:10.1021/acs.nanolett.6b03488.
- [8] E. M. T. Fadaly, A. Dijkstra, J. R. Suckert, D. Ziss, M. A. J. van Tilburg, C. Mao, Y. Ren, V. T. van Lange, K. Korzun, S. Kölling, M. A. Verheijen, D. Busse, C. Rödl, J. Furthmüller, F. Bechstedt, J. Stangl, J. J. Finley, S. Botti, J. E. M. Haverkort, E. P. A. M. Bakkers, Direct-bandgap emission from hexagonal Ge and SiGe alloys, *Nature* 580 (7802) (2020) 205–209. doi:10.1038/s41586-020-2150-y.
- [9] C. Rödl, J. Furthmüller, J. R. Suckert, V. Armuzza, F. Bechstedt, S. Botti, Accurate electronic and optical properties of hexagonal germanium for optoelectronic applications, *Phys. Rev. Mater.* 3 (3) (2019) 034602. doi:10.1103/PhysRevMaterials.3.034602.
- [10] C. Rödl, T. Sander, F. Bechstedt, J. Vidal, P. Olsson, S. Laribi, J.-F. Guillemoles, Wurtzite silicon as a potential absorber in photovoltaics: Tailoring the

- optical absorption by applying strain, *Phys. Rev. B* 92 (4) (2015) 045207. doi:10.1103/PhysRevB.92.045207.
- [11] J. Bandet, B. Despax, M. Caumont, Vibrational and electronic properties of stabilized wurtzite-like silicon, *J. Phys. D* 35 (3) (2002) 234–239. doi:10.1088/0022-3727/35/3/311.
- [12] B. Haberl, M. Guthrie, B. D. Malone, J. S. Smith, S. V. Sinogeikin, M. L. Cohen, J. S. Williams, G. Shen, J. E. Bradby, Controlled formation of metastable germanium polymorphs, *Phys. Rev. B* 89 (14) (2014) 144111. doi:10.1103/PhysRevB.89.144111.
- [13] H. I. T. Hauge, M. A. Verheijen, S. Conesa-Boj, T. Etzelstorfer, M. Watzinger, D. Kriegner, I. Zardo, C. Fasolato, F. Capitani, P. Postorino, S. Kölling, A. Li, S. Assali, J. Stangl, E. P. A. M. Bakkers, Hexagonal Silicon Realized, *Nano Lett.* 15 (9) (2015) 5855–5860. doi:10.1021/acs.nanolett.5b01939.
- [14] J. L. Morán-López, F. Mejía-Lira, J. M. Sanchez (Eds.), *Structural and Phase Stability of Alloys*, Springer, Boston, MA, 1992. doi:10.1007/978-1-4615-3382-5.
- [15] S. Conesa-Boj, H. I. T. Hauge, M. A. Verheijen, S. Assali, A. Li, E. P. A. M. Bakkers, A. Fontcuberta i Morral, Cracking the Si Shell Growth in Hexagonal GaP-Si Core-Shell Nanowires, *Nano Lett.* 15 (5) (2015) 2974–2979. doi:10.1021/nl504813e.
- [16] E. M. T. Fadaly, A. Marzegalli, Y. Ren, L. Sun, A. Dijkstra, D. de Matteis, E. Scalise, A. Sarikov, M. De Luca, R. Rurali, I. Zardo, J. E. M. Haverkort, S. Botti, L. Miglio, E. P. A. M. Bakkers, M. A. Verheijen, Unveiling planar defects in hexagonal group iv materials, submitted (2021).
- [17] X. Cartoixà, M. Palummo, H. I. T. Hauge, E. P. A. M. Bakkers, R. Rurali, Optical Emission in Hexagonal SiGe Nanowires, *Nano Lett.* 17 (8) (2017) 4753–4758. doi:10.1021/acs.nanolett.7b01441.
- [18] G. Kresse, J. Furthmüller, Efficient iterative schemes for *ab initio* total-energy calculations using a plane-wave basis set, *Phys. Rev. B* 54 (16) (1996) 11169–11186. doi:10.1103/PhysRevB.54.11169.
- [19] G. Kresse, D. Joubert, From ultrasoft pseudopotentials to the projector augmented-wave method, *Phys. Rev. B* 59 (3) (1999) 1758–1775. doi:10.1103/PhysRevB.59.1758.
- [20] J. P. Perdew, A. Ruzsinszky, G. I. Csonka, O. A. Vydrov, G. E. Scuseria, L. A. Constantin, X. Zhou, K. Burke, Restoring the Density-Gradient Expansion for Exchange in Solids and Surfaces, *Phys. Rev. Lett.* 100 (13) (2008) 136406. doi:10.1103/PhysRevLett.100.136406.
- [21] G. I. Csonka, J. P. Perdew, A. Ruzsinszky, P. H. T. Philipsen, S. Lebègue, J. Paier, O. A. Vydrov, J. G. Ángyán, Assessing the performance of recent density functionals for bulk solids, *Phys. Rev. B* 79 (15) (2009) 155107. doi:10.1103/PhysRevB.79.155107.
- [22] G.-X. Zhang, A. M. Reilly, A. Tkatchenko, M. Scheffler, Performance of various density-functional approximations for cohesive properties of 64 bulk solids, *New J. Phys.* 20 (6) (2018) 063020. doi:10.1088/1367-2630/aac7f0.
- [23] S. P. Ong, W. D. Richards, A. Jain, G. Hautier, M. Kocher, S. Cholia, D. Gunter, V. L. Chevrier, K. A. Persson, G. Ceder, Python Materials Genomics (pymatgen): A robust, open-source python library for materials analysis, *Comput. Mater. Sci.* 68 (2013) 314–319. doi:10.1016/j.commatsci.2012.10.028.
- [24] F. Tran, P. Blaha, Accurate band gaps of semiconductors and insulators with a semilocal exchange-correlation potential, *Phys. Rev. Lett.* 102 (2009) 226401. doi:10.1103/PhysRevLett.102.226401. URL <https://link.aps.org/doi/10.1103/PhysRevLett.102.226401>
- [25] P. Borlido, T. Aull, A. W. Huran, F. Tran, M. A. L. Marques, S. Botti, Large-scale benchmark of

- exchange–correlation functionals for the determination of electronic band gaps of solids, *J. Chem. Theory Comput.* 15 (9) (2019) 5069–5079. doi:10.1021/acs.jctc.9b00322. URL <https://doi.org/10.1021/acs.jctc.9b00322>
- [26] M. Laubscher, S. Kufner, P. Kroll, F. Bechstedt, Amorphous Ge quantum dots embedded in crystalline Si:ab initio results, *J. Phys. Condens. Matter* 27 (40) (2015) 405302. doi:10.1088/0953-8984/27/40/405302.
- [27] C. Delerue, G. Allan, M. Lannoo, Theoretical aspects of the luminescence of porous silicon, *Phys. Rev. B* 48 (15) (1993) 11024–11036. doi:10.1103/PhysRevB.48.11024.
- [28] D. Dexter, *Theory of the optical properties of imperfections in nonmetals*, in: F. Seitz, D. Turnbull (Eds.), *Solid State Physics*, Vol. 6, Academic Press, 1958, p. 353. doi:10.1016/S0081-1947(08)60730-4. URL <http://www.sciencedirect.com/science/article/pii/S0081194708607304>
- [29] G. Jellison, T. Haynes, H. Burke, Optical functions of silicon-germanium alloys determined using spectroscopic ellipsometry, *Opt. Mater.* 2 (2) (1993) 105–117. doi:10.1016/0925-3467(93)90035-Y.
- [30] A.-B. Chen, A. Sher, *Semiconductor Alloys: Physics and Materials Engineering, Microdevices*, Plenum Press, New York, 1995. doi:10.1007/978-1-4613-0317-6.
- [31] A. Sher, M. van Schilfhaarde, A.-B. Chen, W. Chen, Quasichemical approximation in binary alloys, *Phys. Rev. B* 36 (8) (1987) 4279–4295. doi:10.1103/PhysRevB.36.4279.
- [32] A. van de Walle, M. Asta, G. Ceder, The alloy theoretic automated toolkit: A user guide, *Calphad* 26 (4) (2002) 539–553. doi:10.1016/S0364-5916(02)80006-2.
- [33] L. Vegard, Die Konstitution der Mischkristalle und die Raumfüllung der Atome, *Z. Physik* 5 (1) (1921) 17–26. doi:10.1007/BF01349680.
- [34] H. I. T. Hauge, S. Conesa-Boj, M. A. Verheijen, S. Koelling, E. P. A. M. Bakkers, Single-Crystalline Hexagonal Silicon–Germanium, *Nano Lett.* 17 (1) (2017) 85–90. doi:10.1021/acs.nanolett.6b03488.
- [35] O. Rubel, A. Bokhanchuk, S. J. Ahmed, E. Assmann, Unfolding the band structure of disordered solids: From bound states to high-mobility Kane fermions, *Phys. Rev. B* 90 (11) (2014) 115202. doi:10.1103/PhysRevB.90.115202.
- [36] L.-W. Wang, L. Bellaiche, S.-H. Wei, A. Zunger, “Majority Representation” of Alloy Electronic States, *Phys. Rev. Lett.* 80 (21) (1998) 4725–4728. doi:10.1103/PhysRevLett.80.4725.
- [37] W. Setyawan, S. Curtarolo, High-throughput electronic band structure calculations: Challenges and tools, *Comput. Mater. Sci.* 49 (2) (2010) 299–312. doi:10.1016/j.commatsci.2010.05.010.
- [38] J. R. Suckert, C. Rödl, J. Furthmüller, F. Bechstedt, S. Botti, Efficient strain-induced light emission in lonsdaleite germanium, *Phys. Rev. Mater.* 5 (2021) 024602. doi:10.1103/PhysRevMaterials.5.024602. URL <https://link.aps.org/doi/10.1103/PhysRevMaterials.5.024602>
- [39] P. Tronc, Y. E. Kitaev, G. Wang, M. F. Limonov, A. G. Panfilov, G. Neu, Optical Selection Rules for Hexagonal GaN, *Phys. Status Solidi B* 216 (1) (1999) 599–603. doi:10.1002/(SICI)1521-3951(199911)216:1<599::AID-PSSB599>3.0.CO;2-H.